JOURNAL OF SOLID STATE CHEMISTRY 33, 403–411 (1980)

Investigation of the Surface Composition of NiO–MgO Solid Solutions by X-Ray Photoelectron Spectroscopy

A. CIMINO,*, B. A. DE ANGELIS,† G. MINELLI,* T. PERSINI,† AND P. SCARPINO†

* *Centro di studio CNR Struttura e Attività Catalitica di Sistemi di Ossidi, Istituto di Chimica Generale e Inorganica, Università, Roma, Italy;*
† *Laboratori Ricerche di Base, ASSORENI, 00015 Monterotondo, Roma, Italy*

Received March 30, 1979; in revised form October 10, 1979

The surface composition of NiO–MgO solid solutions has been investigated by XPS. It has been found that no appreciable deviation from bulk composition is present, or, if present, it goes in the direction of a slight depletion in Ni^{2+} ions at the surface. The approximations involved and the problems encountered in the determination of the surface composition of air-exposed oxide samples are discussed.

Introduction

Oxide solid solutions have been used as a means of investigating several aspects of the problems encountered in heterogeneous catalysis, such as the role of the interactions between active metal ions (hence the collective vs localized properties), the influence of the site symmetry, and the role of the matrix ions. Several papers and some reviews have discussed this approach, describing in particular the catalytic activity of solid solutions of transition metal ions (tmi) toward simple reactions (*1–3*).

The approach based on oxide solid solutions raises a fundamental question: does the surface composition really mirror the bulk composition? In fact any attribution of activity per ion, or any correlation of activity with tmi concentration, requires a knowledge of the actual surface composition. X-Ray photoelectron spectroscopy (XPS or ESCA) which provides a means of directly inspecting surfaces has been widely used for metal alloys (*4*), in relation to catalytic problems, but it has been used much less for oxide systems. Furthermore, some limitations or critical aspects of the application of the technique should be kept in mind before reaching significant conclusions, as contamination present on the surface can simulate or dissimulate surface enrichment effects (*5*). The present paper reports the results for the NiO–MgO system. This system is of particular interest because the catalytic activity for N_2O decomposition per Ni^{2+} ion decreases with increasing nickel concentration, a feature exhibited by several other tmi oxide solid solutions for the same reaction (*1*). The desirability of a check of the surface composition is then apparent, to exclude any major segregation on the surface which might simulate a high activity per ion in the

0022-4596/80/090403-09$02.00/0

diluted specimens. Furthermore the NiO–MgO system shows practically ideal thermodynamic behavior (*6*), and therefore gives an interesting opening to the study of the correlation between bulk and surface properties.

Experimental

Preparation and Chemical Analysis

The pure oxide NiO was prepared by calcination of the carbonate for several hours at 900 or 1000°C. Pure MgO was prepared by calcination of the basic carbonate $MgCO_3 \cdot Mg(OH)_2 \cdot 3H_2O$ at 900, 1000, or 1200°C. In several cases a further treatment at 800°C for 3 hr just before recording the spectra was performed, for both NiO and MgO. Reagent-grade chemicals were used.

The solid solutions were prepared by impregnating MgO, obtained by calcination of basic carbonate at 600°C for 5 hr, with the appropriate amount of nickel nitrate solution, of such a concentration as to keep the solid and the liquid volumes comparable. After digestion, the paste was dried at 110°C, ground, calcined at 600°C for 3 hr, ground, and finally calcined in air at 1200°C for 5 hr, except for the most concentrated specimens, which received an additional calcination treatment to check whether bulk homogeneity had been achieved. Some specimens of high surface area were prepared according to the procedure of Hagan *et al.* (*7*). Their features are included in Table I.

The solid solutions are designated by the symbol MN, followed by a figure giving the nominal nickel content expressed as Ni atoms per 100 Mg atoms. The high surface area specimens are marked HSA.

Chemical analyses of nickel were carried out by atomic absorption, the calibration curve being obtained from standards containing magnesium. The concentrations hereafter specified refer to the actual chemical content. Table I lists the specimens and their properties.

TABLE I

SOLID SOLUTIONS (MN) SPECIMENS AND THEIR PROPERTIES

Sample	Ni molar fraction (x_{Ni})	Lattice parameter a (Å)
MN 1	0.010	4.2109
MN 5[a]	0.048	4.2089
	0.051	4.2094
	0.051	4.2096
MN 10	0.095	4.2077
MN 15	0.132	4.2072
MN 20	0.177	4.2039
MN 30[a]	0.245	4.2.16
	0.239	4.2018
MN 50[a]	0.329	4.1982
	0.356	4.1977
MN 70	0.399	4.1962
MN 90	0.469	4.1942
MN 100	0.514	4.1927
MN 110	0.563	4.1908
MN 5 HSA[b]	0.032	—
MN 30 HSA[c]	0.191	—
MN 50 HSA[d]	0.264	—

[a] More than one value of a and x_{Ni} is given when independent preparations are involved.

[b] Surface Area (SA) = 129 $m^2\ g^{-1}$. Water content c_{H_2O} = 18.4%.

[c] SA = 82 $m^2\ g^{-1}$ (r.t. outgassing), 87 $m^2\ g^{-1}$ (480°C outgassing), c_{H_2O} = 7.6%.

[d] SA = 71 $m^2\ g^{-1}$ (r.t. outgassing), 84 $m^2 g^{-1}$ (480°C outgassing), c_{H_2O} = 3.6%.

X-Ray Analysis

The specimens were tested for the absence of spurious phases and of unreacted oxides by film powder diffraction (Straumanis technique). The lattice parameter a was measured to an accuracy of $\pm 1 \times 10^{-4}$ Å by an extrapolation technique (*8*). The a values fit the earlier data from this laboratory (*8*) and confirm the linear variation of a with the nickel molar fraction x_{Ni}.

X-Ray Photoelectron Spectroscopy Measurements

XPS measurements were carried out with an AEI ES 100 spectrometer, with AlKα excitation (1486.6 eV). The powders were pressed into a trough, 1 to 2 mm deep and 6×15 mm^2 area, on a gold-plated metallic backing, in such a way that the gold on the backing was completely covered by the specimen. The vacuum was about 10^{-6} Torr.

The following peaks were recorded: Ni($2p_{3/2}$) (625 eV), O(1*s*) (955 eV), C(1*s*) (1200 eV), Mg(2*p*) (1435 eV), Mg($K_1L_2L_2$) (1180 eV). The figures in parentheses give the kinetic energy. Some measurements involved the total Ni(2*p*) peak. Care was taken to record the peaks at constant intervals of time and in the same order, and to repeat the measurement at least once. The intensity of the peaks other than C showed a decrease with time, most marked for the Ni peak.

The samples were calcined for 3 hr at 800°C in air, just before recording the spectra. For the pure oxides, MgO and NiO, this procedure was occasionally omitted to study the influence of lack of conditioning. Intensity values were obtained by measuring the area under the peak. For the Ni($2p_{3/2}$) the problem arises of the choice of the baseline. To get correct values of the intensity one should take into account the main peaks ($2p_{3/2}$, $2p_{1/2}$), their shake-up satellites, and the inelastic losses. Even recording the spectrum over a 50-eV range it is not possible to include all inelastic losses, and therefore there is no certainty of obtaining 100% of the intensity, without unduly increasing the recording time. There are, however, several procedures which allow a measurement of a constant fraction of the total intensity (*9*). The one we have adopted consists of drawing a baseline which includes the $2p_{3/2}$ peak and its shake-up satellite, but not the $2p_{1/2}$ peak (Fig. 1).

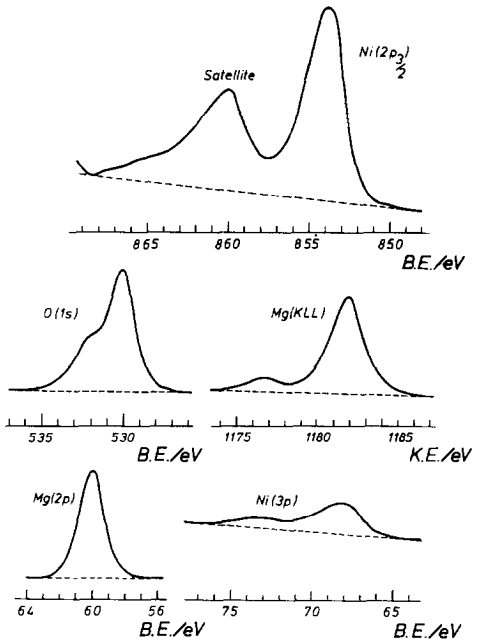

FIG. 1. Peaks of Ni, Mg, and O for which the intensity was determined.

Figure 1 also shows the baseline used for the other peaks.

The O(1*s*) peak shows two components, a stronger one assigned to O^{2-}, and a weaker one at about 2 eV higher BE, which can be assigned to OH^-, adsorbed water, or carbonate species (*5*). A deconvolution of the peak into the two components has been carried out. The relative ratio of the two components did not vary much throughout the series, provided that the conditioning of 800°C was done. The presence of a small amount of carbonate can be seen from the carbon 1*s* peak.

Results and Discussion

As a preliminary remark one can note that the escape depth of the Ni(2*p*) is low enough and sufficiently different from that of Mg(2*p*) to allow the detection of a significant surface segregation, as suggested by comparison with the ZnO–MgO system (*5*).

The measurement of the relative intensity of two peaks arising from nickel and magnesium, that is, the I_{Ni}/I_{Mg} ratio, is perhaps the simplest way to test for surface composition. As noted (*5*), deviation from linearity of I_{Ni}/I_{Mg} vs x_{Ni}/x_{Mg} can be taken as an indication of deviation of surface composition from bulk composition, but it is not an absolute proof, since contamination effects can vary with composition. On the other hand, the linearity of plots such as I_{Ni}/I_{Mg} vs x_{Ni}/x_{Mg} or I_{Ni} vs x_{Ni} is not a guarantee of equality between surface and bulk composition, since the former can follow the latter in a way which is effectively linear, without being equal to it. It is necessary therefore to check the experimental values of the intensity ratios against the values expected for the case where $x^s_{Ni} = x^b_{Ni}$.

The definition of the expected values for the intensity ratios requires a calibration which involves the pure oxides. The oxygen peak O(1*s*) can be utilized as an internal standard for eliminating random errors. The check is conveniently made by plotting the ratios $(I_{Ni}/I_{Mg})_{MN}$ measured in the MN samples against x_{Ni}/x_{Mg}, and by comparing them to values expected if $x^s_{Ni} = x^b_{Ni}$, which in the same plot lie on a straight line. In order to trace this line, the ratios I_{Ni}/I_O and I_{Mg}/I_O are first determined in the pure oxides. The straight line is then fixed by the value of $(I_{Ni}/I_O)_{NiO}/(I_{Mg}/I_O)_{MgO}$ which should be observed at $x_{Ni}/x_{Mg} = 1$. The ratios I_{Ni}/I_O and I_{Mg}/I_O are therefore an essential basis for the subsequent check, and reproducibility of their values has been tested for specimens prepared under the same conditions, but in independent preparations, as well as for specimens for which the preparation conditions were somewhat changed.

One remark concerns the adoption of oxygen as an internal standard. As noted, the O(1*s*) peak results from two components: the O^{2-} at low BE values, and the OH^- (or H_2O) at high BE values. The relative intensity of the two components did not vary much. After some checks, it was found that the O^{2-} component gave more reproducible results, and was therefore generally adopted. The use of the total O(1*s*) intensity did not, however, affect the results appreciably. It should also be noted that because of the experimental error in the determination of the $(I_{Mg}/I_O)_{MgO}$ and $(I_{Ni}/I_O)_{NiO}$ ratios, the reference line admits a spread which is independent of the intrinsic error of the measurement of each MN sample. In order to show the spread, the confidence limits for 99% confidence interval (see, e.g., (*10*)) have been traced in the graphs as broken lines.

Different peaks arising from Ni^{2+} and Mg^{2+} ions can be selected, and the results based on Ni($2p_{3/2}$) and Mg(2*p*) are shown in Fig. 2. One can see that the experimental values tend to be lower than expected. If significant, the result would point to an enrichment of magnesium in the outer

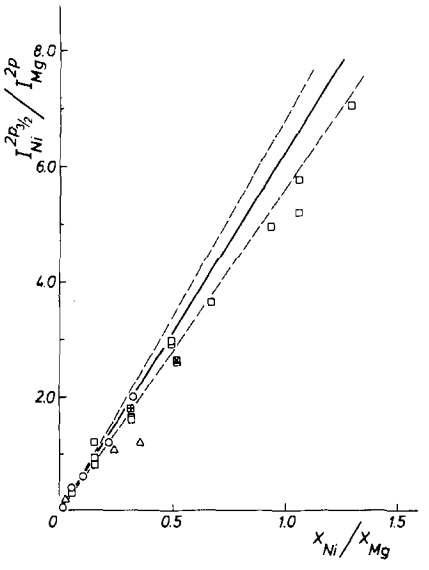

FIG. 2. Intensity ratio Ni($2p_{3/2}$)/Mg(2*p*) vs molar fraction ratio. The solid reference line was obtained from pure oxides; the broken lines indicate the expected spread at the 99% confidence level (see text). ⊠ and ⊞ indicate samples treated in H_2 and CO_2, respectively.

layers, but in view of the experimental error of each point (not drawn for the sake of clarity) the deviation might not be really significant.

A plot of $I^{2p_{3/2}}_{Ni}/I^{KLL}_{Mg}$ (not reported) is practically equal to Fig. 2, showing that the scatter and the tendency to lie below the reference line mainly arise from the Ni($2p_{3/2}$) peak.

In view of the much lower escape depth for electrons from Ni($2p$) (λ = 10 Å) than from Ni($3p$) (λ = 19 Å), one would expect that in passing from Ni($2p$) to Ni($3p$) the deviation from the corresponding expected line would tend to decrease. This proposition has been tested, but the confidence limits for the expected ratios I^{3p}_{Ni}/I^{2p}_{Mg} are wider, in view of the larger errors made in evaluating the intensity of the Ni($3p$). As Fig. 3 shows, the experimental points tend to be spread within the confidence limits of the expected value. In summary, graphs based on the I_{Ni}/I_{Mg} ratios lend support to a very slight enrichment of magnesium in the outer layers.

A different way of testing is to make

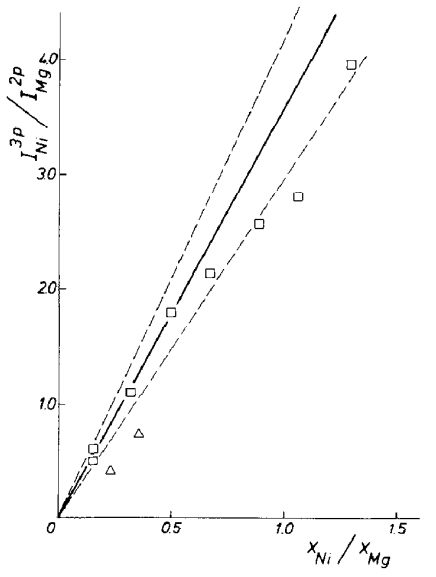

FIG. 3. Intensity ratio Ni($3p$)/Mg($2p$) vs molar fraction ratio.

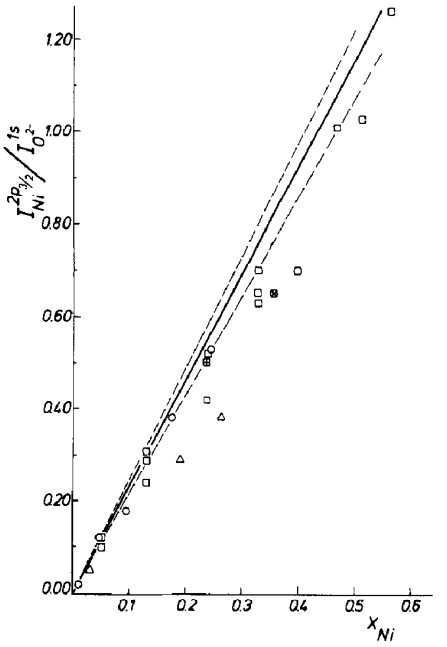

FIG. 4. Intensity ratio Ni($2p_{3/2}$)/O^{2-}($1s$) vs Ni molar fraction.

direct use of the intensity ratio between nickel and oxygen peaks measured in the MN samples, $(I_{Ni}/I_O)_{MN}$. The ratio is compared to that expected for each specimen if $x^s_{Ni} = x^b_{Ni}$, the expected ratio being calculated from the value measured for pure NiO. Figure 4 gives the plot of $I^{2p_{3/2}}_{Ni}/I^{1s}_{O^{2-}}$, and shows that the measured ratios tend to be low as compared to the expected values, which is represented by the solid line (broken lines are as before the confidence limits for the reference line). There is again an indication of a slight enrichment in magnesium in the outer layers. The testing by means of the peak Ni($3p$) is shown in Fig. 5. As for Fig. 3, the spread is now within the confidence limits of the reference line.

So far all checks presented were made using the O^{2-} component of the O($1s$) peak as an internal standard for normalization of the cation intensities. As already quoted, the results are not much affected if the total peak intensity is taken into account. By way of illustration, Fig. 6 shows the situa-

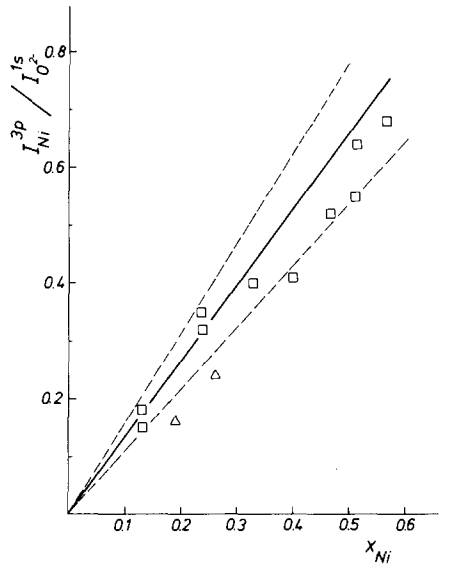

FIG. 5. Intensity ratio Ni(3p)/O^{2-}(1s) vs Ni molar fraction.

tion for the plot, analogous to Fig. 4, of the ratio $I^{2p_{3/2}}_{Ni}/I^{1s}_{O}$ vs x_{Ni}. A slight tendency for the ratio to be low is maintained; the scatter, however, is larger, and is probably not significantly outside the confidence limits. With regard to the oxygen peak, it should be noted that undoubtedly the surface is contaminated by hydroxides, and perhaps carbonates (see remarks on the C peak). If the hydration is larger on MN samples than on pure NiO, as one would expect (see HSA specimens below), a comparison of the Ni/O peak intensity in MN samples to that of NiO could introduce an error. The error, however, would simulate an enrichment of nickel, because as the surface is hydroxylated, hence depleted of O^{2-} ions in MN samples, the ratio $I_{Ni}/I_{O^{2-}}$ should appear larger. The points in the graphs would therefore be moved upward. The opposite having been observed, the apparent magnesium enrichment cannot be due to a simple variation of the available oxide ion concentration. A further argument could be given on the effect of surface hydration, namely, that the contamination is larger on MN samples than it is on NiO, and therefore the Ni(2p) peak is more attenuated than the Mg peaks, without, however, implying any real variation of composition of the surface layer of the solid solution with respect to the bulk.

So far the analysis has been based on the nickel peaks, and it is therefore useful to turn to the Mg peaks, because they should show a tendency opposite to that of the Ni peaks, and they can therefore be used as a check. Figure 7 plots $I^{2p}_{Mg}/I^{1s}_{O^{2-}}$ vs x_{Ni}, and shows no tendency for any enrichment in magnesium. The same conclusion can be drawn from Fig. 8, which plots in a similar way the Auger transition Mg(KLL). Thus the complementary analysis of the Mg peaks does not provide any evidence for magnesium enrichment.

As a final way of testing for surface homogeneity with the bulk Fig. 9 is presented. The figure plots Σ_I vs x_{Ni} where

$$\Sigma_I = \frac{(I^{2p_{3/2}}_{Ni}/I^{1s}_{O^{2-}})_{MN}}{(I^{2p_{3/2}}_{Ni}/I^{1s}_{O^{2-}})_{NiO}} + \frac{(I^{2p}_{Mg}/I^{1s}_{O^{2-}})_{MN}}{(I^{2p}_{Mg}/I^{1s}_{O^{2-}})_{MgO}}$$

has the value of unity only if homogeneous

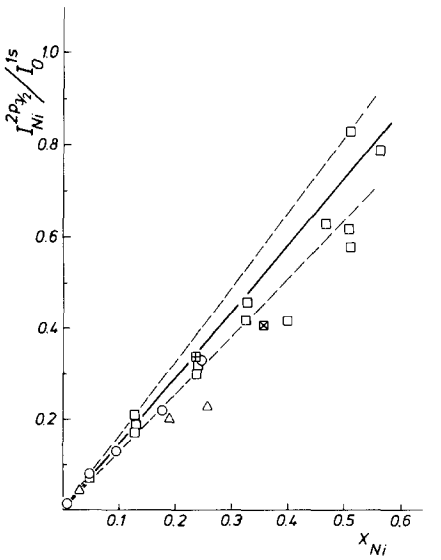

FIG. 6. Intensity ratio Ni($2p_{3/2}$)/O(1s) vs Ni molar fraction.

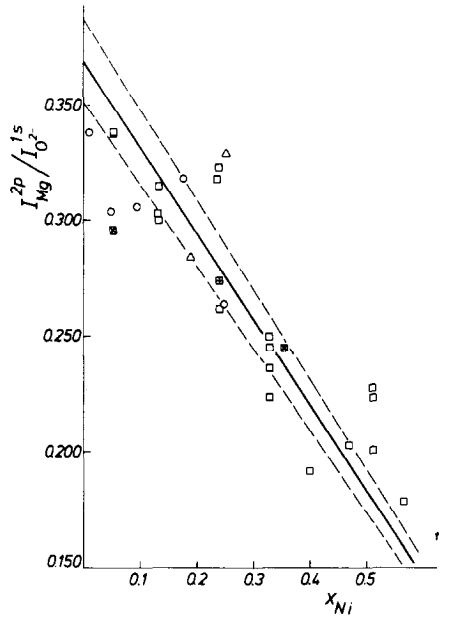

FIG. 7. Intensity ratio (Mg(2*p*)/O^{2-}(1*s*) vs Ni molar fraction.

(*11*), since the escape depths for the electrons involved in the two peaks considered are different. It is lower than unity if depleted in nickel or if a depletion can be simulated for reasons which have been mentioned. It can be seen that the majority of the points are within the experimental error of the value $\Sigma_I = 1$, and a significance test shows that in spite of the tendency of the points to be low, the upper confidence limit is just the value unity.

It is appropriate to remark that we have assumed that the escape depth in our sample does not significantly change with the Ni content. This assumption seems reasonable also in consideration of the fact that all our samples have the same crystal structure.

Effect of Gas Treatment

The influence of a hydrogen treatment was studied by submitting the specimen to a flow of gas (1 atm, 400°C) outside the spectrometer, cooling in hydrogen, and immediate transfer into the spectrometer. Two specimens were studied, MN 5 and MN 50, and both failed to show any variation of position or of relative intensity of the Ni peaks. The intensity data are reported in the graphs of Figs. 2, 4, and 6–9, only for MN 50, to avoid overcrowding in the low x_{Ni} region. The carbon contamination was observed to decrease by this treatment. The O(1*s*) peak was not affected, and the ratio of the low to high BE components was not altered in a significant way.

The results indicate that no reduction, followed by metal particle growth and segregation takes place. In fact, even if the exposure to air had resulted in rapid oxidation, an enrichment of nickel (due to the oxide formed) would have been observed. It can be noted, however, that the results do not exclude a reduction limited to the outside layer: its influence on the spectrum could escape experimental observation, and furthermore a rapid reoxidation upon exposure to air could restore the initial state.

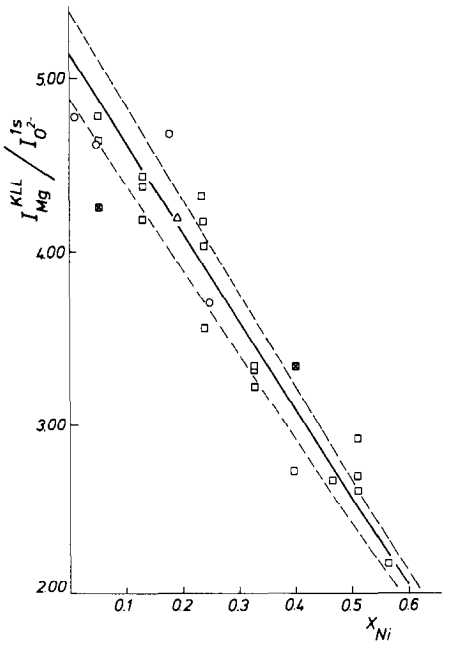

FIG. 8. Intensity ratio Mg(*KLL*)/O^{2-}(1*s*) vs Ni molar fraction.

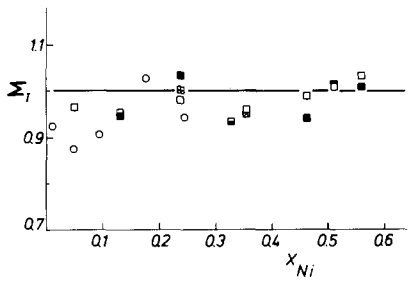

FIG. 9. Sum (Σ_I) of the Ni and Mg intensity ratio between the solid solution values and the pure oxide values vs Ni molar fraction (Σ_I is defined in the text).

Treatment with CO_2 (1 atm, 250°C) also failed to produce significant changes in the spectrum. In particular, neither the O/C ratio nor the Ni/O ratio varied, showing that carbonate formation, if any, is limited to the outside layers, already contaminated (Figs. 2, 4, and 6–9).

High Surface Area (HSA) Specimens

The results on some high surface area (HSA) specimens are included in the graphs, marked by an open triangle. A lowering of the I_{Ni}/I_{Mg} and I_{Ni}/I_O intensity ratios is observed, while the I_{Mg}/I_O ratio is not significantly altered. These specimens seem to confirm the trend shown by the low area specimens, namely, a possible simulation of Ni depletion due to surface contamination. A significant analysis directed toward the study of the surface/volume ratio would, however, require more stringent control of the atmosphere.

Expected Equilibrium Surface Behavior of the NiO–MgO System

The system ZnO–MgO, previously investigated, showed that the results could be interpreted on the basis of thermodynamic equilibrium between surface and bulk, even though the influence of surface contamination could have been superimposed on it (*5*). It is then appropriate to see the predictions of the thermodynamic model for the system NiO–MgO.

If thermodynamic equilibrium between surface and bulk is achieved, and if the influence of the atmosphere is negligible, one can relate the surface composition to the bulk composition through the surface energy values of the component oxides (*5, 11, 12*). While the value σ_{MgO} is known (1.2 J m^{-2}), that of NiO has not been reported. A rough estimate of σ_{NiO} required to assess whether it is comparable to or less than σ_{MgO} can be made by the adoption of an indirect method. The formula given by Glauberman for ionic solids (*13, 14*), $\sigma = 0.0124\ (Ze)^2/r^3$, where Ze is the ionic charge and r is the interionic distance, gives a good estimate of σ for MgO (1.2 against 1.2, found). The value calculated for FeO (1.1 J m^{-2}) is definitely larger than that measured (0.7) (*12*). It is therefore reasonable to think that the true value for NiO, a compound similar to FeO in several respects, should be appreciably lower than that calculated (1.25). One is therefore led to conclude that $\sigma_{NiO} < \sigma_{MgO}$. On this basis one would expect an enrichment in Ni^{2+} ions on the surface of the solid solutions.

Another thermodynamic approach, suggested by Burton and Machlin for alloys (*15*) but applicable to oxide solid solutions as well, would lead to the same result. In fact, the method is based on the phase diagram of the binary system, and predicts the surface enrichment of that component which lowers the melting point. On the basis of the diagram NiO–MgO (*6*) one would then predict nickel enrichment at the surface.

One is led to conclude that the system is "frozen" at the state of the high-temperature preparation, where surface enrichment predicted on equilibrium considerations is lower, and moreover one can state that the small variations of surface composition, if any, are dictated by chemical reactions with the atmosphere rather than by thermodynamic equilibrium between surface and bulk. In this regard, it is of interest to recall that the free energy of formation of either hydroxides or carbonates of magnesium, if

compared to those of nickel, are such as to favor the reactivity of magnesium ions with respect to nickel ions (ΔG_f (kcal mole^{-1}): MgO, −136; $Mg(OH)_2$, −199; $MgCO_3$, −246; NiO, −52; $Ni(OH)_2$, −108; $NiCO_3$, −147).

Concluding Remarks

The analysis of the XPS data shows in detail that isolated determinations of peak intensities can lead to erroneous results. This is particularly true for powder systems, where contamination of the surface can be more severe. However, it is possible to draw a picture of the surface composition through an analysis of several peaks and of the trend shown for several intensity ratios as a function of composition, thus exploiting the difference of escape depth values, internal standards, and checks on the complementary behavior of both components in a binary system.

With regard to the NiO–MgO system, one can exclude appreciable deviation of surface composition from bulk composition in spite of the limitations imposed by the assumptions made on λ (independence from the matrix composition) and by the averaging effect of the probing depths.

The variation of the catalytic activity per ion with nickel concentration is therefore real, even though some very limited deviation cannot be excluded. In fact evidence for a slight deviation, of the order of 10%, might be present, but it could be simulated by contamination effects. The deviation, if present, is in the direction of a slight depletion in Ni^{2+} ions at the surface. The results show that the surface composition is not controlled by the thermodynamic parameters of surface energy, but rather by the influence of the atmosphere and of the ensuing chemical reactions. A comparison with the ZnO–MgO system is then significant. For the latter, in spite of the possible role of surface reactions (hydroxide or carbonate formation) the thermodynamic parameters of the pure oxides are still dominating the behavior of the system. In NiO–MgO the thermodynamic parameters of the pure oxides are overwhelmed by other processes. It is of interest to recall that in the case of ZnO–MgO the preference for more open structures (tetrahedral vs octahedral) as well as size considerations parallels the thermodynamic tendency for zinc enrichment in the surface, while in the case of NiO–MgO, site preference (octahedral) and size effects (Ni^{2+} insertion shrinks the lattice parameter, hence the Mg^{2+} ion is slightly larger) tend to maintain the nickel ions inside the MgO structure, thus opposing thermodynamic considerations of the pure oxides, and paralleling the influence of surface reactions.

References

1. A. Cimino, *Chim. Ind. (Milan)* **56**, 27 (1974).
2. F. S. Stone, *J. Solid State Chem.* **12**, 271 (1975).
3. G. K. Boreskov, *in* "Proceedings, 6th International Congress on Catalysis, London, 1976," p. 204. The Chemical Society, London, 1977.
4. W. M. H. Sachtler and R. A. Van Santen, *in* "Advances in Catalysis," Vol. 26, p. 69, Academic Press, New York (1977).
5. A. Cimino, B. A. De Angelis, and G. Minelli, *J. Electron Spectrosc.* **13**, 291 (1978).
6. W. C. Hahn, Jr., and A. Muan, *J. Phys. Chem. Solids* **19**, 339 (1961).
7. A. P. Hagan, C. O. Arean, and F. S. Stone, *in* "Reactivity of Solids" (J. Wood, O. Lindqvist, C. Helgesson, and N. G. Vannerberg, Eds.), p. 69, Plenum, New York (1977).
8. A. Cimino, M. Lojacono, P. Porta, and M. Valigi, *Z. Phys. Chem. N.F.* **55**, 14 (1967).
9. C. J. Powell and P. E. Larson, *Appl. Surface Sci.* **1**, 186 (1978).
10. M. R. Spiegel, "Theory and Problems of Statistics," McGraw–Hill, New York (1961).
11. G. A. Somorjai and S. H. Overbury, *Faraday Disc. Chem. Soc.* **60**, 279 (1975).
12. S. H. Overbury, P. A. Bertrand, and G. A. Somorjai, *Chem. Rev.* **75**, 547 (1975).
13. A. E. Glauberman, *Zh. Fiz. Khim.* **23**, 124 (1949).
14. J. J. Gilman, *J. Appl. Phys.* **31**, 2208 (1960).
15. J. J. Burton and E. S. Machlin, *Phys. Rev. Lett.* **37**, 1433 (1976).